Mine Water Environ
DOI 10.1007/s10230-016-0427-z

TECHNICAL ARTICLE

Characterization of Two Nanofiltration Membranes for the Separation of Ions from Acid Mine Water

Oluranti Agboola[1,2] · Touhami Mokrani[1] · Emmanuel Rotimi Sadiku[2] · Andrei Kolesnikov[2] · Olubiyi Isola Olukunle[2] · Johannes Phillippus Maree[3]

Received: 11 March 2016 / Accepted: 16 December 2016

Abstract We evaluated nanofiltration for separation of ions from acid mine drainage (AMD), using two composite nanofiltration membranes (Nano-Pro-3012 and NF90) as examples of the polyamide class of acid-stable membranes. The structure of the NF membranes was characterized by scanning electron and atomic force microscopy. The NF90 displayed a higher permeate flux than Nano-Pro-3012, with higher relative roughness at both pH values. Both membranes suitably rejected most of the metals found in the AMD, but the Nano-Pro-3012 membrane proved unsuitable for sulphate removal.

Keywords Toxic contaminants · Pore size · Surface roughness · Solute rejection · Flux

Introduction

Most conventional methods of treating acid mine drainage (AMD) are combine lime neutralization and precipitation and settling of the precipitates in ponds. The most commonly used commercial process is the high-density sludge (HDS) process (Pondja et al. 2014; Zinck and Griffith 2000), in which a portion of the settled metal precipitates (sludge) is recycled to the AMD treatment tank. Membrane treatment by nanofiltration (NF) and reverse osmosis (RO) are also well established treatment techniques for ion removal because they are efficient, easy to operate, do not require much space, and can attain strict discharge criteria (Fu and Wang 2011). Several studies have successfully used membrane separation to treat AMD (Al-Zoubi et al. 2010; Juby 1992; Morgan et al. 2001; Mortazavi and Chaulk 2012; Rieger et al. 2009).

NF and RO technologies are designed, manufactured, and built for the removal of salts and dissolved ions, not for particulate matter. However, mine water often contains particulate matter as well as organic substances and other solids that may not be compatible with RO and NF membrane processes. Therefore, proper pretreatment to remove particulates and any scale-forming contaminants is important to membrane performance and life span. Roughing filters, which are mainly physical filters, can be used to pre-treat the AMD, since they efficiently separate fine solid particles for prolonged periods without chemical addition (Nkwonta 2010). Stand-alone microfiltration (MF) and ultrafiltration (UF) processes, or a hybrid integration step, can be used to efficiently separate suspended particles and macromolecules as a pretreatment step to NF or RO membranes.

Nanofiltration membranes display separation characteristics in the intermediate range between RO and UF (Lin et al. 2007), with a pore size of about 0.001 μm. A UF membrane has a pore size around 0.01 μm, while reverse osmosis membranes have a pore size of about 0.0001 μm. In concept and operation, NF is much the same as RO; the key difference is the degree of removal of monovalent ions such as chlorides. NF membranes require considerably less pressure (5–40 bars) than RO, leading to significant energy

Electronic Supplementary Material The online version of this article (doi:10.1007/s10230-016-0427-z) contains supplementary material, which is available to authorized users.

✉ Oluranti Agboola
funmi2406@gmail.com

[1] Department of Civil and Chemical Engineering, University of South Africa, Johannesburg, South Africa

[2] Department of Chemical, Metallurgical and Materials Engineering, Tshwane University of Technology, Pretoria, South Africa

[3] Phillert Trust, Pretoria, South Africa

Published online: 18 January 2017

savings. The cut-off of NF molecular mass is between 150 and 1000 daltons (Da). Due to charge interactions with the NF membranes, multivalent ions are also well retained by NF membranes. The rejection of a solute in NF is a function of the physical constraints of molecular pore size and thermodynamic limitations, electrostatic interactions, and dispersion forces (Gregor 1976; Hanemaaijer et al. 1989; Reiss 2005). The durability and effectiveness of nanofiltration membranes in the operational environment depends on the thermal, mechanical, and chemical properties of the membrane polymer, which may be quantified by membrane characterization (Agboola et al. 2014; Khulbe et al. 2008). It is therefore important to understand the surface properties of membranes in order to know which nanofiltration membrane should be used in a particular separation process. The objective of this study was to test the performance of a particularly acid-stable NF membrane (Nano-Pro-3012) and compare it with another commercial chemically stable NF membrane (NF90) for AMD treatment.

Materials and Experimental Methods

Nanofiltration Membranes

Two composite nanofiltration membranes (Nano-Pro-3012 and NF90) were chosen for this research, as representative of a class of membranes that are acid-stable in water treatment applications. The Nano-Pro-3012 membrane was provided by Bio Pure Technology; the NF90 membrane was provided by Dow-Filtec, South Africa. Both are polyamide thin film composite membranes. Their operating properties, as provided by the manufacturers, are provided in Supplementary Table 1.

Water Sample

The AMD was sampled from the Gauteng Western basin region, South Africa (Supplementary Fig. 1). The approximate composition of the contaminants in the AMD solution at the original pH of 3.09 is listed in Table 1. The water sample was filtered to remove suspended particulates before it was acidified to a pH of 2.2 for the experiments by titrating it with hydrochloric acid (HCl). The primary purpose for lowering the pH was to reduce the potential of scaling during filtration, but it also allowed us assess the effect a low pH would have on ion rejection. Hydrochloric acid was used instead of sulphuric acid because of an initial plan to measure sulphate concentrations along with the other ions. The approximate chlorine concentration in the solution at pH 2.2 was 121 mg/L.

Table 1 Approximate chemical composition and concentrations of ions in the AMD

Metals	Composition (mg/L)
Ca^{2+}	800
Fe^{2+}	600
Mg^{2+}	120
Na^{+}	100
Mn^{2+}	100
Al^{3+}	50
Ni^{2+}	4
Co^{2+}	2
SO_4	3500
Fe^{3+}	750

Analytical Method

The concentrations of solutes (cations) in the feed and permeate were measured using inductively coupled plasma optical emission spectro (ICP-OES) Arcos with the torch position in radial view. The analysis of anions was performed on a Metrohm 883 basic ion chromatograph (IC) plus from Switzerland. The solution pH and temperature were measured using a pH meter (Mettler Toledo FG20) and a thermometer, respectively.

Laboratory Dead-end Test Cell

The investigation was done using a Memcon Laboratory stirring cell (see Supplementary Fig. 2). A membrane with an active area of ≈0.01075 m^2 was fitted to the cell. A litre of solution (distilled water or AMD) was placed in the cell at the product inlet, and then pressure was applied via nitrogen gas. The permeate was collected and its mass was determined.

Filtration Experiments

The membrane sheet was initially rinsed with distilled water and the clean water flux (CWF) was measured prior to the AMD experiment. The membranes were compacted for 3 days at the manufacturers' recommended operating pressures to stabilize the membranes by filtering distilled water until no further flux decline was observed. This compression process ensured that impurities were removed from the system and that flux declines observed during the experiments were due to membrane fouling and not membrane compaction. This was also the reason for operating at a constant pressure.

The CWF experiments were done at a stirring velocity of 500 rpm, at a temperature of 25 °C and a pressure of 10 bar

to ascertain whether membrane fouling would occur. Due to the different pore sizes of the membranes, experiments with different membrane samples were not run for the same length of time. Membrane compaction experiments were conducted for 360 and 180 min for Nano-Pro-3012 and NF90, respectively. Samples were taken from the feed and permeate every 30 min for analysis. After the AMD filtration was terminated, the membrane was cleaned with distilled water, followed by a clean water flux measurement to ascertain if the membranes had fouled.

Analysis of Results

The permeate flux and rejection were investigated as a function of parameters such as operating time and water recovery. The observed rejection, which is the measure of how well a membrane retains a solute, was calculated by Eq. 1:

$$\%R = \left(1 - \frac{C_p}{C_i}\right) \times 100 \tag{1}$$

where C_p and C_i are the solution concentrations in the permeate and initial feed solution, respectively. The permeate flux Jv (L/m^2/h) was determined by measuring the volume of permeate collected in a given time interval divided by the membrane area (A) per Eq. 2:

$$J_v = \frac{Q}{A} \tag{2}$$

where Q represents the flow rate of the permeate.

Scanning Electron Microscopy (SEM)

A scanning electron microscope (SEM; Joel field emission electron microscope JESM-7600F) was used to visualize the surfaces of the membranes. The virgin and used membranes were mounted on a double sided carbon tape and the surfaces were coated with about a 5 nm thickness of iridium in order to make it conductive for the SEM studies. The sample was exposed to an electron beam at an accelerating voltage of 15 KV to get a signal for the SEM studies. The micro-marker on the micrographs was used to estimate the pore size (diameter).

Atomic Force Microscopy (AFM)

Clean membranes were cut into small pieces and glued onto a sample holder with agar tape before noncontact AFM imaging was performed using an Agilent Technologies 5500 scanning probe microscope (PicoPlus-Atomic Force Microscopy Series 5500). The AFM cantilever used was made out of silicon (Nano-sensors) with a resonant frequency of about 60 kHz, a nominal spring constant of 7.4 N m^{-1} with a typical tip radius of less than 7 nm. The AFM measurements were performed on dry membranes in an air atmosphere with a relative humidity of about 30%. The AFM images were flattened with order 1 and the RMS (root-mean squared) value of the roughness was obtained by using the Nanotechnology Research Tool (Horcas et al. 2007). The roughness depends on the scan size; therefore, a comparative analysis was required so that the roughness would be obtained from images with the same scan areas (Khulbe et al. 2008). The AFM was done for the 1.0×1.0 μm^2 scan area.

Scanning Probe Microscope Image Process—Roughness Analysis

The membrane roughness was further analyzed with WXSM 5.0 software, a freeware scanning probe microscopy software based on MS-Windows (Horcas et al. 2007). The surfaces of the NF membranes were compared in terms of roughness parameters, which depend on the curvature and the size of the AFM tip and the treatment of the captured surface data (plane fitting, flattering, filtering, etc.). The roughness parameter, *RMS*, is a statistical measure of the relative roughness of a surface and is essentially the standard deviation of the heights for all the pixels in the image from the arithmetic mean. The *RMS* of the roughness varies with the interval range; it is given by the following expression:

$$RMS = \sqrt{\frac{\sum_{ij} \left(a_{ij} - \langle a \rangle\right)^2}{N}} \tag{3}$$

where a_{ij} is the height of a particular point on the image (U + 212B), a is the average/mean height of all the pixels in the image (U + 212B), and N is the total number of pixels within the image. The maximum range is the height difference between the lowest and highest pixels in the image. The mean height of the pixel was calculated as the arithmetic average of the pixels' height. The mean roughness is the mean value of the surface relative to the centre plane (a plane that divides the volumes enclosed by the image in half), which is given by the average height (<a>) of the pixel in the image:

$$\langle a \rangle = \frac{\sum_{ij} a_{ij}}{N} \tag{4}$$

Results and Discussions

SEM Analysis

The surface structure and pore sizes of the membrane samples were examined by SEM (Fig. 1). The Nano-Pro-3012

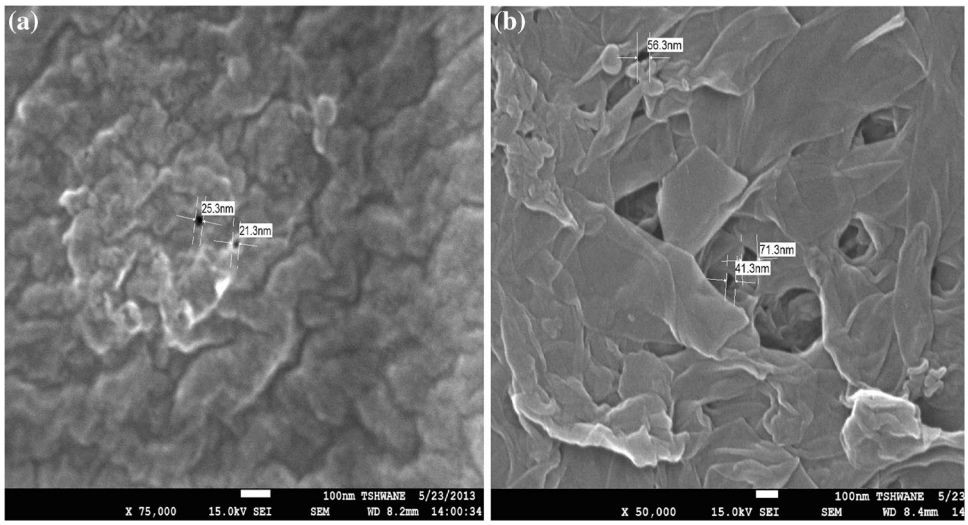

Fig. 1 SEM image of: **a** Top surface of Nano-Pro-3012, **b** Top surface of NF90

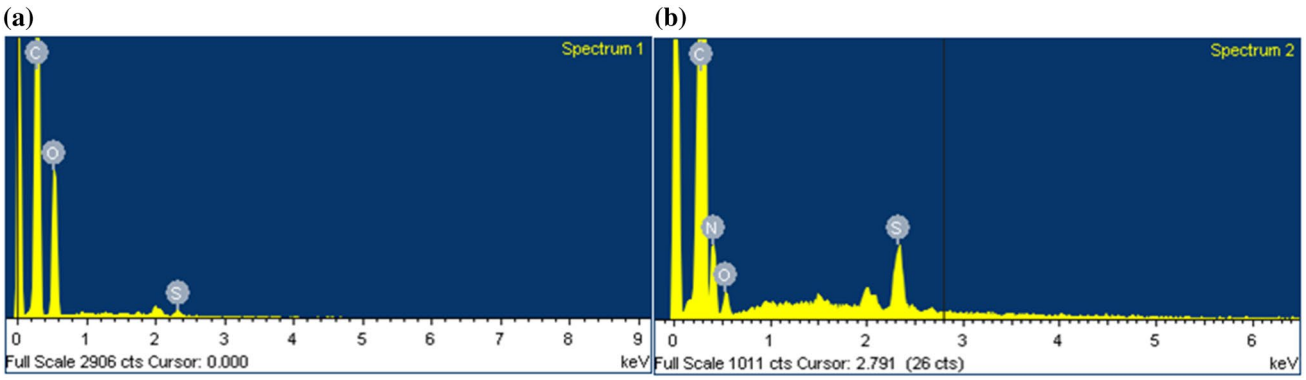

Fig. 2 EDXA spectra of, **a** clean Nano-Pro-3012 and **b** clean NF90

membrane appears to be smooth, dense, and compact with few visible pores. The NF90 membrane had larger pores and an intertwining fibrous network structure with numerous pores. Figure 2 shows the energy dispersive X-ray analysis (EDXA) line profile of the clean NF membranes. The membranes are entirely made of carbon (Supplementary Table 2); the presence of nitrogen, oxygen, and silicon on the surface of both membranes reflects the presence of organic matter. The elemental composition, which is given in both atomic percent and weight percent, reflects the amount of a particular element in the analysed volume. The sum of atomic weight for all of the elements was normalized to 100%.

AFM Analysis

Surface roughness can be used to predict membrane performance because it is proportional to the bond strength of the membrane. The greater the roughness, the greater the adhesive strength of the membrane; thus greater efficiency will be achieved in the separation process (Bowen et al. 1998). The surface roughness of the membranes was compared for identical scan sizes due to the effect of image size on roughness parameters. The AFM image of a 1.0×1.0 μm^2 scan area was used to examine the topography and to determine roughness. Figure 3 shows that the orthographic images of the top surface of both membranes, with information on the depth of the membranes in the Z-direction. The 3D orthographic image of NF90 shows a network-like fibrous structure and thick peaks and valleys. These thick peaks are responsible for the higher roughness of NF90. The 3D orthographic image of Nano-Pro-3012 shows a denser structure and higher ridges. WXSM 5.0 software gave the statistical roughness parameters that were used to quantitatively describe the surface roughness of the membranes (1×1 μm^2 scan areas). NF90 had a higher surface

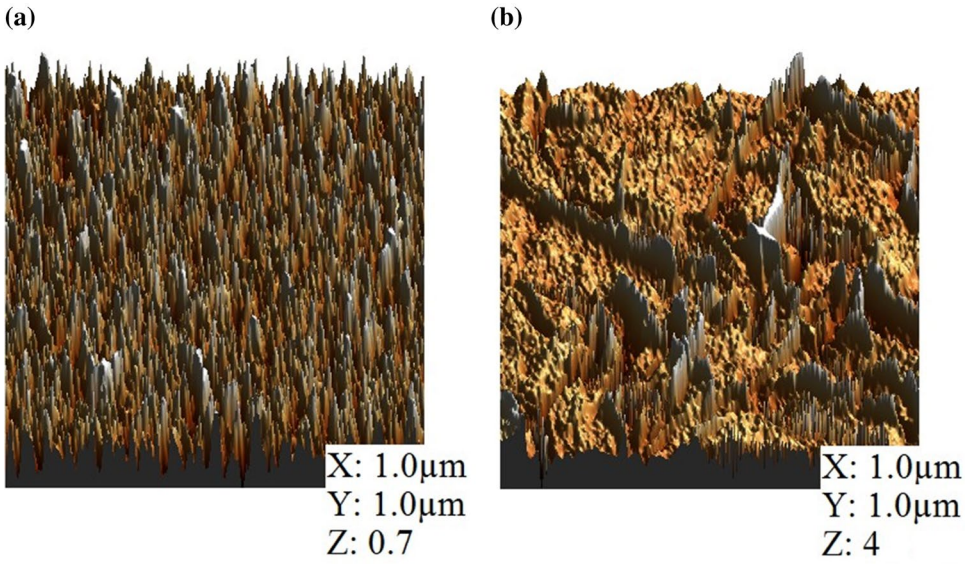

Fig. 3 Three dimensional active surface of, **a** Nano-Pro-3012 and **b** NF90 membranes obtained by non-contact mode AFM

roughness (0.621 Å) and mean roughness (0.402 Å) than Nano-Pro-3012, which had a surface roughness and mean roughness 0.17 and 0.134 Å, respectively. In comparison NF90 was rougher than Nano-Pro-3012.

Membrane Porosity

By measuring the dependence of the membrane's pure water flux at constant pressure, the membrane's active layer porosity can be characterized, since the clean water fluxes depend on the pore size of the membranes (Fig. 4). The results agreed with the SEM characterizations. The membranes were compacted over time due to the high feed pressure, which decreased permeate flux. The degree of compaction depends on the membrane type and feed pressure (Chin et al. 2002).

Percentage of Solute Concentration Rejected

Both membranes gave better rejection at the higher pH 3.09 (Table 2); this is because fewer unwanted solute particles are transferred through membranes at higher pH values (Xia et al. 2006). Another reason for better rejection at higher pH is because more fouling occurs at the lower pH, which is governed by the interplay between chemical and physical (hydrodynamic) interactions (Hong and Elimelech 1977). Previous studies have shown that organic fouling was most severe at low pH, high ionic strength, and particularly with the presence of calcium (Manttari et al. 2000; Yuan and Zydney 2000). NF90 gave better rejection of sulphate at both pH values (2.2 and 3.09). It was observed that the water recovery

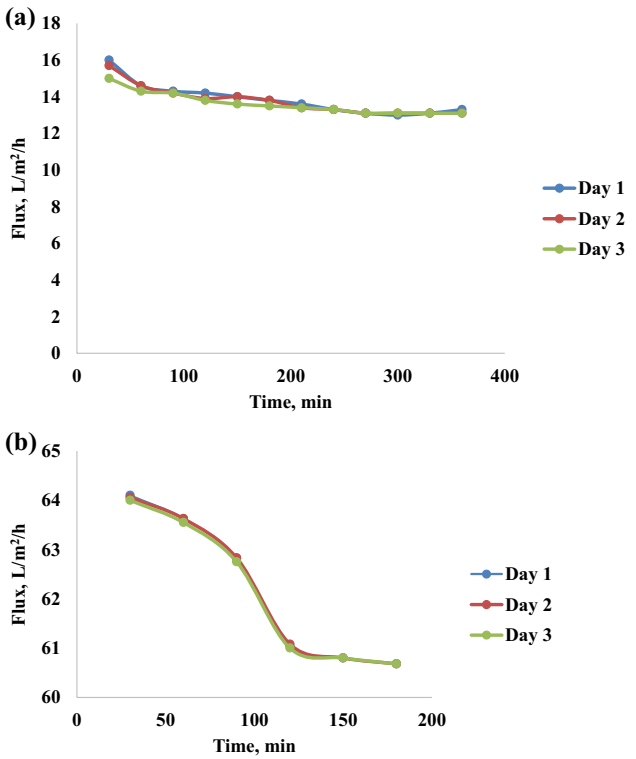

Fig. 4 Flux of distilled water as function of time, **a** Nano-Pro-3012 and **b** NF90

percentage of Nano-Pro-3012 was higher at the higher pH, while NF90 showed the opposite result. This is as a result of the membrane structure, which depends on pH. Nano-Pro-3012 could experience pore enlargement at the higher pH, which could be due to stronger electrostatic

Table 2 Summary of the average rejection of ions from the AMD solution

Ions	Nano-Pro-3012		NF90	
	% Rejection at pH 3.09	% Rejection at pH 2.2	% Rejection at pH 3.09	% Rejection at pH 2.2
Fe	98.0	93.0	97.0	95.4
Mn	98.0	90.3	96.3	88.6
Mg	98.0	91.3	96.2	89.0
Ni	100.0	90.1	98.0	77.7
Co	98.8	88.8	93.2	90.0
Ca	96.0	95.2	98.0	95.5
Na	74.0	63.0	95.0	93.0
Al	83.0	80.2	82.0	79.0
SO_4	86.0	86.3	96.4	97.6
Cl	52	46	55	51

repulsions between the dissociated functional groups of the membrane material (Berg et al. 1997).

Flux During AMD Filtration

The dead-end filtration of the AMD shows that filtration capacity decreases with time due to clogging. Figure 5 shows that the retained AMD particles build up on the membrane surfaces and within the membranes, thereby reducing permeate flux. Figure 6 shows the percent water recovery of the two nanofiltration membranes as a function of flux and the influent pH. The particles built up, resulting in an increased resistance to filtration, thus causing the permeate flux to decline and reducing water recovery (Fig. 6). Relative roughness (r) is a useful parameter to indicate spatial heterogeneity; hence, Fig. 7 shows the relationship between flux and relative roughness. After obtaining a 3D image for the surface roughness, the data matrix of the surface roughness was copied from the WXSM 5.0 software. The flux was plotted against the roughness obtained from the data matrix.

This result can be attributed to the larger pore size of the NF90 membrane compared to that of the Nano-Pro-3012 membrane; as a result, the NF90 membrane had greater permeate flux and relative roughness than the Nano-Pro-3012 membrane at both pH values. It was observed that the surface characterization was associated with permeation properties; the lower the value of roughness, the lower the flux and the higher the rejection.

Filtration Performance

In order to investigate fouling and verify the permeability of the two NF membranes, a clean water flux experiment

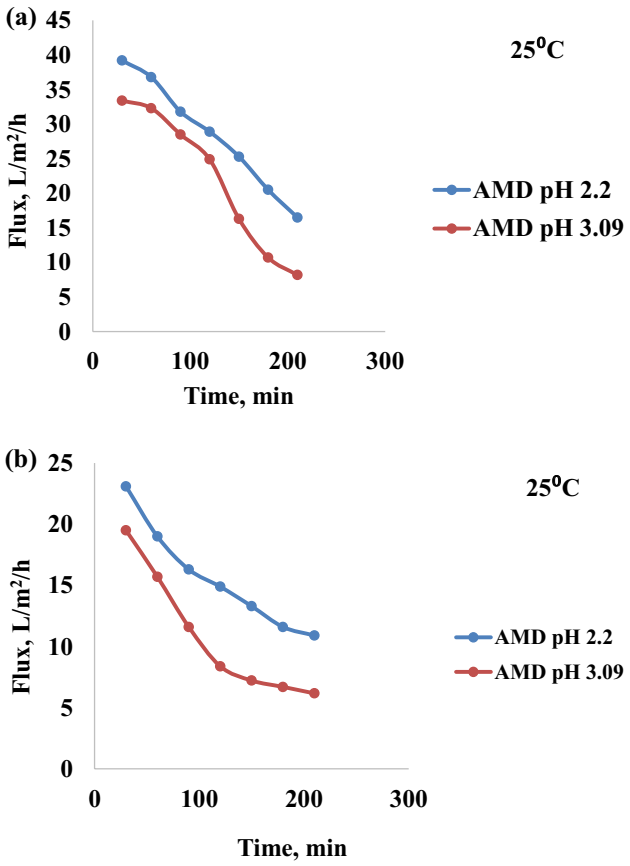

Fig. 5 Flux during AMD filtration for, **a** NF90 and **b** Nano-Pro-3012 at 10 bars

was conducted after each AMD experiment and compared with the initial clean water flux (Supplementary Fig. 3). The initial clean water flux was higher than after exposure of the membranes to the AMD, which indicates that the membrane surface was affected by the AMD at pH 2.2 and 3.09. Therefore, the AMD should be adequately pretreated, perhaps by microfiltration or ultrafiltration, before the use of NF to prevent membrane fouling.

EDX Analysis of the Fouled NF Membranes

Figure 8 shows the EDXA line profile of the fouled NF membranes. The presence of Fe, Al, Cu, SO_4, Mg on the surface of Nano-Pro-3012 and the presence of Al, Ca, Cu, and SO_4 on the surface of NF90 indicates the deposition of cations and anion on the surface of the membranes. Thus, the foulant on the membranes consists of both cations and anions. The elemental composition of the two membranes is given in Supplementary Table 3.

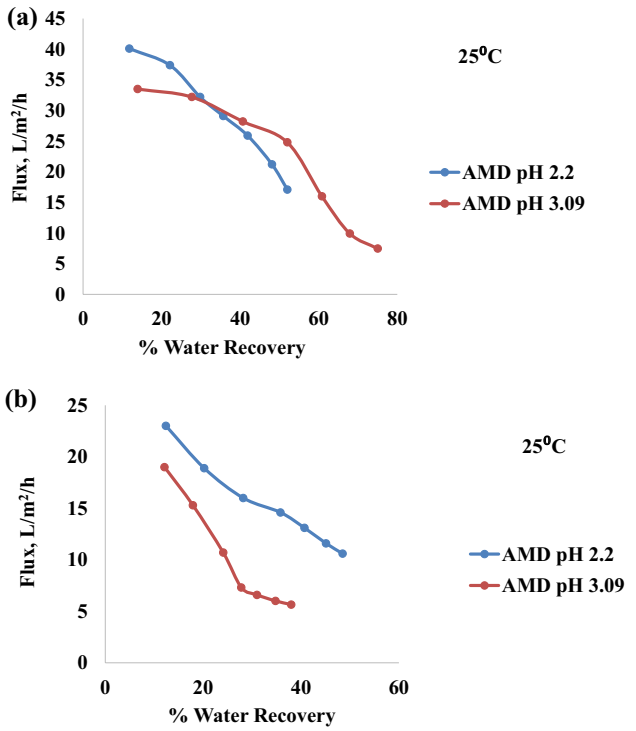

Fig. 6 Flux as a function of % water recovery during AMD filtration for, **a** NF90 and **b** Nano-Pro-3012 at 10 bars

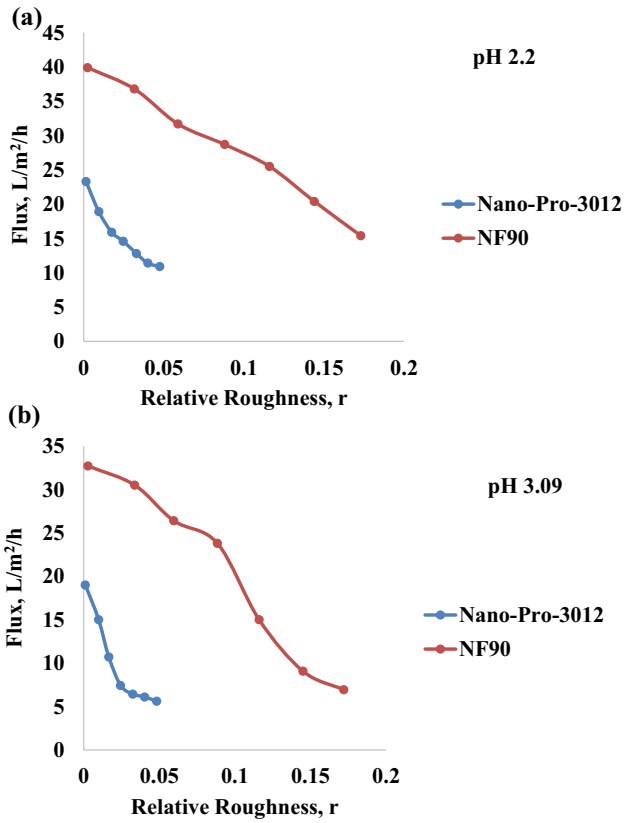

Fig. 7 Flux as a function of relative roughness, **a** pH 2.2, **b** pH 3.09

Cleaning of Membranes

After filtration of the AMD at the two different pHs, the membranes were cleaned to see if their initial performance would recover. First, the reversible part of the flux decline was removed by rinsing the membranes with distilled water (Weis et al. 2003). Then, a chemical cleaning method was used to remove the irreversible part of the fouling: the membranes were soaked in HCl for 10 min, after which a CWF was determined. Supplementary Figure 4 shows the CWF before and after the experiments, and after membrane cleaning. The membrane fouling of NF90 was completely removed by the cleaning, while Nano-Pro-3012 was only partially restored. If the two nanofiltration membranes would be implemented in the future for the treatment of AMD, care should be taken to pretreat the mine water properly prior to treatment to prevent membrane fouling.

Conclusion

This laboratory study investigated the performance of two acid-stable NF membranes for potential treatment of mine-influenced water streams. Attention was given to the relationship between the permeate flux, percent water recovery, and relative roughness. Particle build-up on the membranes increased resistance to filtration, which decreased permeate flux and reduced water recovery. It was observed that the surface morphology of the membranes affected the permeation properties; a lower roughness factor decreased the flux and increased the rejection rate. The clean water flux of both membranes decreased after exposure of the membranes to AMD.

Understanding the relationship between membrane performance and solution characteristics is very important for an optimal implementation of the membranes for AMD treatment. The NF membranes both removed most metal ions from the AMD; however, Nano-Pro-3012 did not effectively remove sulphate. Also, pre-treatment of the AMD would prove to be necessary to prevent fouling of either NF membrane.

Based on our results, future investigations should include: modelling and simulation using the extended Nernst-Plank equation in conjunction with Darcy's law to better predict the rejection of metals at different pH values to improve performance and treatment of different effluents.

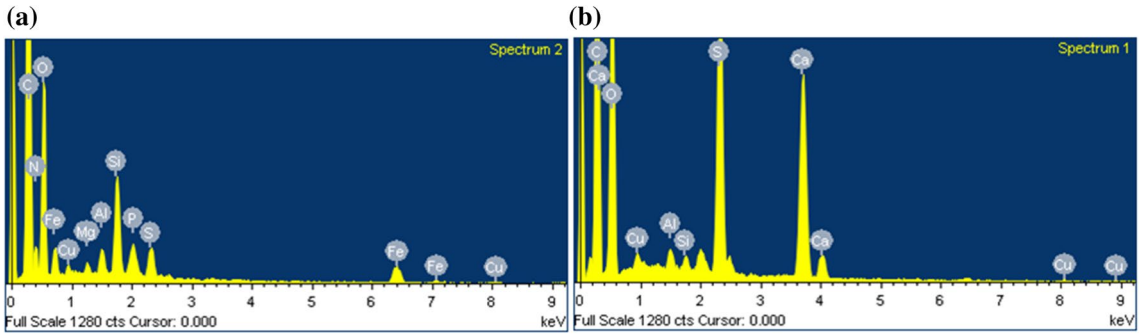

Fig. 8 EDXA spectra of, **a** fouled Nano-Pro-3012 and **b** fouled NF90

References

Agboola O, Maree J, Mbaya R (2014) Characterization and performance of nanofiltration membranes: a review. Environ Chem Lett 12:241–255

Al-Zoubi H, Rieger A, Steinberger P, Pelz W, Haseneder R, Härtel G (2010) Optimization study for treatment of acid mine drainage using membrane technology. Sep Sci Technol 45:2004–2016

Berg P, Hagmeyer G, Gimbel R (1997) Removal of pesticides and other micropollutants by nanofiltration. Desalin 113:205–208

Bowen WR, Hilal N, Lovitt RW, Wright CJ (1998) A new technique for membrane characterization: direct measurement of the force of adhesion of a single particle using atomic force microscopy. J Membr Sci 139:269–274

Chin TD, Black BD, Perry SAL (2002) Implementation of arsenic treatment systems, part 2: design considerations, operation, and maintenance. AWWA Research Foundation and American Water Works Assoc, Washington DC

Fu F, Wang Q (2011) Removal of heavy metals ions from waste water: a review. J Environ Manage 92:407–418

Gregor HP (1976) Fixed-charge ultrafiltration membranes. In: Sélégny E (ed), Charge Gels and Membranes, Ch 11, R. Reidel Publ Co, Dordrecht

Hanemaaijer JH, Robbertsen T, Van Den Boomgaard TH, Gunnick JW (1989) Fouling of ultrafiltration membranes: the role of protein adsorption and salt precipitation. J Membr Sci 40:199–217

Hong S, Elimelech M (1977) Chemical and physical aspects of natural organic matter (NOM) fouling of nanofiltration membranes. J Membr Sci 132(2):159–181

Horcas I, Fernandez R, Gomez-Rodriguez JM, Colchero J, Gomez-Herrero J, Baro AM (2007) WSXM: a software for scanning probe microscopy and a tool for nanotechnology. Rev Sci Instrum 78:013705–013708

Juby GJG (1992) Membrane desalination of service water from gold mines. J SA Inst Miner Metall 9:65–69

Khulbe KC, Feng CY, Matsuura TS (2008) Synthetic Polymeric Membranes Characterization by Atomic Force Microscopy. Springer-Verlag, Berlin

Lin SW, Sicairos SP, Navarro RMF (2007) Preparation, characterization and salt rejection of negatively charged polyamide nanofiltration membranes. J Mex Chem Soc 51:129–135

Manttari M, Puro L, Nuortila-Jokinen J, Nyström M (2000) Fouling effects of polysaccharides and humic acid in nanofiltration. J Membr Sci 165:1–17

Morgan BE, Loewenthal RE, Lahav O (2001) Fundamental study of a one-step ambient temperature ferrite process for treatment of acid mine drainage waters. Water SA 27:277–282

Mortazavi S, Chaulk J (2012) Treatment of acid mine drainage streams using membrane separation. In: Price WA, Hogan C, Tremblay G (eds), Proc, 9th International Conf on Acid Rock Drainage, Ottawa, ON, Canada

Nkwonta PI (2010) Roughing filters: an alternative passive pre-treatment of coal mine water in South Africa. MS thesis, Dept of Civil Eng, Tshwane Univ of Technology

Pondja EA, Persson KM, Matsinhe NP (2014) A survey of experience gained from the treatment of coal mine wastewater. J Water Resource Prot 14(6):1646–1658

Reiss CR (2005) Mechanisms of nanofilter fouling and treatment alternatives for surface water supplies. PhD thesis, Dept of Civil and Environ Eng, Univ of Central Florida Orlando, FL, pp 32–33

Rieger A, Steinberger P, Pelz W, Haseneder R, Härtel G (2009) Mine Water treatment by membrane filtration processes-experimental investigation on applicability. Desalin Water Treat 6:54–60

Weis A, Bird MR, Nyström M (2003) The chemical cleaning of polymeric UF membranes fouled with spent sulphite liquor over multiple operational cycles. J Membr Sci 216:67–79

Xia S, Dong B, Zhang Q, Xu B, Gao N, Causseranda C (2006) Study of arsenic removal by nanofiltration and its application in China. Desalin 204:374–379

Yuan W, Zydney AL (2000) Humic acid fouling during ultrafiltration. Environ Sci Technol 34:5043–5050

Zinck JM, Griffith WF (2000) An assessment of HDS-type lime treatment processes-efficiency and environmental impact. Proc, 5th International Conf on Acid Rock Drainage, Soc of Mining. Metallurgy Exploration 1:1027–1034